Monthly Notices of the ROYAL ASTRONOMICAL SOCIETY

MNRAS **516,** 4650–4659 (2022) https://doi.org/10.1093/mnras/stac2574
Advance Access publication 2022 September 11

Group velocity of obliquely propagating Alfvén waves in a magnetized dusty plasma

L. B. De Toni ,★ R. Gaelzer ★ and L. F. Ziebell★

Instituto de Física, Universidade Federal do Rio Grande do Sul, CP 15051, 91501-970 Porto Alegre, RS, Brazil

Accepted 2022 September 7. Received 2022 September 1; in original form 2022 July 5

ABSTRACT

In this work, we investigate the characteristics of the group velocity of obliquely propagating Alfvén waves in a dusty plasma typical of a stellar wind. The dispersion relation is derived with the aid of the kinetic theory for a magnetized dusty plasma consisting of electrons and ions, with distribution of momenta described by a Maxwellian function. The dust particles are considered to be immobile and have all the same size; they are electrically charged by absorption of plasma particles via inelastic collisions and by photoionization. We numerically solve the dispersion relation and calculate the components of group velocity (along and transverse to the magnetic field) for the normal modes, namely the compressional and shear Alfvén waves (CAW and SAW). The results show that the direction of the group velocity of CAWs is greatly modified with the wave-vector direction. On the other hand, SAWs will present group velocity propagating practically along the magnetic field. The changes in dust parameters, such as number density and equilibrium electrical charge, may significantly change the waves' characteristics. It is seen that for sufficiently high dust to ion number density ratio, the SAWs may present perpendicular group velocity propagating in opposite direction to the perpendicular phase velocity, in a small interval of wavenumber values; we also notice that this interval may change, or even vanish, when the flux of radiation incident on the dust is altered, changing the equilibrium electrical charge of the grains.

Key words: plasmas – waves – methods: numerical – stars: winds, outflows.

1 INTRODUCTION

Space plasmas are commonly populated by dust particles with very high masses relative to an ion, and a wide range of sizes, with radii of the order of nanometres to a few millimetres. These grains of dust will accumulate their own electrical charge, which can be positive or negative, depending on the charging mechanisms and surrounding environment. The presence of an electrically charged population of dust particles can strongly influence the plasma properties, and drive it to behave in a very different manner in comparison with a conventional ion–electron plasma. Another common feature of space plasmas is the presence of Alfvén waves. These low-frequency waves are generated by oscillations of the magnetic field and play important roles in several astrophysical mechanisms, such as the heating and transport of energy in stellar winds, transfer of angular momentum in interstellar molecular clouds, and providing scattering mechanisms for the acceleration of cosmic rays (Cramer 2001).

Numerous theoretical investigations of how these waves might heat and accelerate the solar wind have been proposed (e.g. Barnes 1969; Alazraki & Couturier 1971; Belcher 1971; Belcher & Davis 1971; Heinemann & Olbert 1980; Jatenco-Pereira & Opher 1989; Falceta-Gonçalves & Jatenco-Pereira 2002). This idea is supported by the fact that Alfvén waves were detected in the solar wind, first trough *in situ* observations by the *Mariner 5* spacecraft (Belcher & Davis 1971), and more recently by the *Ulysses* spacecraft near the Earth (Goldstein et al. 1995; Smith et al. 1995). Advances coming from ground-based (Tomczyk et al. 2007) and space-based instrumentation (De Pontieu et al. 2007) provide further evidence of a significant energy flux near the solar corona caused by Alfvén waves.

It was pointed out by Leamon et al. (1999) that purely parallel propagating Alfvén waves are not sufficient to describe the observed characteristics of the solar wind. Some theoretical and observational results suggest that kinetic Alfvén waves (KAW), which are essentially highly oblique Alfvén waves, must play an important role in particle acceleration (Hui & Seyler 1992) and in turbulent processes in the solar wind (Leamon et al. 1998, 2000; Bale et al. 2005). In the kinetic regime, the electron thermal speed is higher than the Alfvén speed and the magnetic-aligned electric field produced by obliquely propagating waves is expected to produce strong wave–particle interactions. For this reason, KAWs are often associated with the heating and acceleration of electrons along the plasma magnetic field lines in solar flares and in aurora arcs (Hasegawa 1976; Goertz & Boswell 1979; Bian, Kontar & Brown 2010).

In uniform plasmas, it is well known that Alfvén waves consist of the compressional and shear Alfvén waves (CAW and SAW) that may also be denominated as, respectively, whistler and ion cyclotron waves in the large wavenumber regime. For parallel propagation, these two waves present null values of parallel electric field and, for a dustless plasma, they couple into a single mode in the short wavenumber region; however, for oblique propagation, these modes no longer couple (Gaelzer et al. 2009). The CAW compresses the

★ E-mail: luan.toni@ufrgs.br (LBDT); rudi.gaelzer@ufrgs.br (RG); luiz.ziebell@ufrgs.br (LFZ)

© 2022 The Author(s)
Published by Oxford University Press on behalf of Royal Astronomical Society

Downloaded from https://academic.oup.com/mnras/article/516/3/4650/6696011 by Universidade Federal do Rio Grande do Sul user on 02 December 2022

magnetic field lines, which acts as a restoring force, and propagates isotropically, with its group velocity along the same direction of its phase velocity (Chen, Zonca & Lin 2021). On the other hand, for SAW, the magnetic field lines twist relative to one another but do not compress. One of the most important properties of SAW is that it is an anisotropic electromagnetic wave, i.e. whilst its phase velocity can propagate in any direction, its group velocity propagates along the magnetic field (Swanson 2003). However, Vásconez et al. (2015) have shown that for dispersive Alfvén waves all modes have a non-vanishing component of the group velocity in the perpendicular direction to the magnetic field, although for SAW it is much less than the parallel component.

A substantial fraction of the Alfvén waves energy flux is transferred to plasma particles by some form of dissipation, being Landau damping the usual process for a dustless plasma. However, several works showed, with the aid of the kinetic theory, that the dispersion relation in a magnetized dusty plasma is greatly modified, with the normal modes showing a stronger damping mechanism than the usual Landau damping, caused by the inelastic collisions that occur between the electrically charged dust grains and plasma particles (see e.g. de Juli et al. 2005, 2007; Ziebell et al. 2008; Gaelzer et al. 2009; Gaelzer, de Juli & Ziebell 2010; De Toni & Gaelzer 2021; De Toni, Gaelzer & Ziebell 2022).

The presence of dust particles near the solar corona has been observed from infrared emissions, especially during solar eclipses (Léna et al. 1974; Mankin, MacQueen & Lee 1974; Dürst 1982; Leinert et al. 1998), providing evidence of dust particles existing as close as $2\,R_\odot$, where $R_\odot$ is the Sun's radius. *In situ* observations by the NASA's *Parker Solar Probe* (Howard et al. 2019) also corroborate the theory that there is a decrease in dust density as it approaches the Sun's surface, since dust grains this close would be heated and vapourized by the intense sunlight. Observations also provide evidence of the existence of dust envelopes around many other stars. Of particular interest is the role that dust particles play in the acceleration mechanism of stellar winds of carbon-rich stars. These stars are notable for losing great amount of their masses by way of these powerful stellar winds (Knapp 1987; Lafon & Berruyer 1991; Mattsson & Höfner 2011). Several models that describe the mass loss in late-type stars show that the stellar winds of these stars are usually dust driven (Bowen 1988; Sandin & Höfner 2003; Woitke 2006; Boulangier et al. 2018), in which stellar photons, incident on dust particles, will lead to a radiative acceleration of the grains away from the star and, subsequently, momentum will be transferred to the surrounding gas by gas–grain collisions. In addition to the radiation pressure, these winds are greatly affected by the strong damping of Alfvén waves, most likely due to grain interaction (Falceta-Gonçalves & Jatenco-Pereira 2002).

In view of the importance of Alfvén waves in the heating and acceleration of dust-driven stellar winds, a substantial amount of work has been done in order to better comprehend the effects of dust particles in the propagation and damping of these waves, which consider purely parallel propagating waves, with dust particles charged only by the absorption of plasma particles (see e.g. de Juli et al. 2005, 2007; Ziebell et al. 2005; Gaelzer et al. 2010). Gaelzer et al. (2009) showed that the dispersion and absorption of obliquely propagating Alfvén waves are also substantially modified by the presence of dust, with the ion cyclotron modes presenting an interval of wavenumber values with null frequency, a feature not observed in a conventional plasma.

Using the formalism developed by Galvão & Ziebell (2012), which includes in the kinetic theory of magnetized dusty plasmas the process of photoionization of dust particles, it is possible to observe the effects caused by the dust population in a more realistic way, since the particles in stellar winds are exposed to radiation coming from the star's surface. In this case, the dust population can present positive values for its electric charge, as opposed to the case where they are charged only by absorption of plasma particles, which tends to negatively charge the dust grains.

De Toni & Gaelzer (2021) first used this formalism to study the changes that the photoionization process may bring to the properties of purely parallel propagating Alfvén waves. Some of the results reveal that the coupling between the whistler and ion cyclotron modes is greatly modified in the large wavelength region once dust particles have null or positive electrical charge. Also, it was shown that the presence of photoionization may greatly modify the damping rates seen in both modes. More recently, De Toni et al. (2022) extended the study of the effects of dust photoionization to obliquely propagating Alfvén waves. It was seen that, for the set of parameters typical of a stellar wind coming from a carbon-rich star, the photoionization process tends to diminish the damping rate of both CAW and SAW modes. Additionally, this charging process reduces the interval of wavenumber values where the SAW presents null frequency.

As mentioned before, both CAW and SAW are expected to present non-zero transverse group velocity, which allow the wave energy to propagate across the magnetic field lines. CAW and SAW waves are known to represent an important mode of energy and momentum transport between the tail of Earth's magnetosphere and the auroral zone (Keiling et al. 2002; Lysak, Song & Jones 2009). In this context the magnitude of the non-vanishing perpendicular group velocity can have important consequences for energy transport, since waves moving along the sheet boundary layer in the magnetotail would also move across the magnetic field lines and leave the plasma sheet boundary layer before reaching the inner magnetosphere (Malovichko 2013).

In non-uniform plasmas in which quantities vary in the direction transverse to the ambient magnetic field causing a large gradient of the Alfvén velocity, waves with small amplitude can undergo phase mixing (Heyvaerts & Priest 1983), in which differences in group velocity at different locations progressively bend wave fronts. Also, waves such as SAW, which have group velocity mostly parallel to the magnetic field, can be subject to resonant absorption, in which case the wave energy concentrates in the local field line where its frequency locally matches a characteristic frequency (Chen & Zonca 1995). However, since SAWs have a non-vanishing perpendicular group velocity, the energy propagates across field lines away from the resonant layer; this mechanism can saturate the growth in amplitude of the resonant oscillation and limit the contraction of its transverse size (Bellan 1994; Stasiewicz et al. 2000). These processes are known to take place in the Earth's magnetosphere and in the Sun's corona, heating and transferring energy to the local plasma (Chen & Hasegawa 1974; Hasegawa & Chen 1976).

Given the importance and ubiquity of phenomena involving wave propagation and energy transfer in space environments, and taking into account that these are commonly populated by dust particles, in this paper, we follow the work of De Toni et al. (2022) by studying the characteristics of the group velocity of oblique Alfvén waves in a dusty plasma typical of a stellar wind environment. The intention is to better understand how the energy of both CAW and SAW propagates in a magnetized dusty plasma and how their group velocity is changed when varying some of the parameters related to the dust particles, such as number density and equilibrium electrical charge.

The structure of this paper is the following. In Section 2, we discuss the plasma model and the dust charging mechanisms considered. In Section 3, the dispersion relation for obliquely propagating Alfvén

Downloaded from https://academic.oup.com/mnras/article/516/3/4650/6696011 by Universidade Federal do Rio Grande do Sul user on 02 December 2022

waves is derived. Section 4 presents the numerical results and discussions. Finally, the conclusions and final remarks are presented in Section 5.

2 THE PLASMA MODEL AND DUST CHARGING PROCESSES

The kinetic formalism applied in this work is the same that recently appeared in De Toni et al. (2022), in which is presented a more detailed account of the theory (see also de Juli & Schneider 1998; de Juli et al. 2005; Gaelzer et al. 2009; Galvão & Ziebell 2012). Nevertheless, it is useful to repeat here some of the basic features of the model.

We start by considering a multicomponent homogeneous plasma consisting of protons, electrons, and spherical dust particles with radius a, placed in an external magnetic field $\boldsymbol{B}_0 = B_0 \boldsymbol{e}_z$ and exposed to anisotropic incidence of radiation, as it happens in the surrounding of stars. Dust grains embedded in a plasma will acquire their own electrical charge by way of many charging processes, which are represented by currents incident on the grains' surface, i.e.

$$\frac{\mathrm{d}q_\mathrm{d}}{\mathrm{d}t} = \sum_k I_k(q_\mathrm{d}), \tag{1}$$

where q_d is the dust electrical charge and I_k is the current correspondent to the kth charging process. After some time, the dust grains will achieve an equilibrium electrical charge $q_{\mathrm{d}0}$, in which case the total current over the surface will be zero, i.e.

$$\left.\frac{\mathrm{d}q_\mathrm{d}}{\mathrm{d}t}\right|_{q_\mathrm{d}=q_{\mathrm{d}0}} = \sum_j I_k(q_{\mathrm{d}0}) = 0. \tag{2}$$

As a consequence of the variable charge of dust particles, the equilibrium number densities $n_{\beta 0}$ of the plasma species β will change through the quasi-neutrality condition:

$$\sum_\beta n_{\beta 0} q_\beta + q_{\mathrm{d}0} n_{\mathrm{d}0} = 0, \tag{3}$$

where q_β is the charge of the plasma species β, and $n_{\mathrm{d}0}$ is the equilibrium density of dust particles.

Generally, in both space and laboratory plasmas, more than one charging process may play an important role in the variation of the dust electrical charge. Some important charging mechanisms that occur on dust particles are: the absorption of plasma particles due to inelastic collisions between them and dust grains; electron emission by photoelectric effect; secondary emission of electrons; thermionic emission; among others. In our model, each of these processes would add an additional term in the kinetic equation of plasma particles and greatly complicate the derivation of the dielectric tensor.

In this work, we consider only the absorption of particles of species β and the photoemission of electrons by the dust grains, represented, respectively, by the currents I_β and I_p. The absorption current is derived from the orbital motion limited (OML) theory (see e.g. Allen 1992; Tsytovich 1997), an approximation valid for weakly magnetized plasmas where the dust particle radius is much smaller than the electron Larmor radius (Chang & Spariosu 1993; Salimullah, Sandberg & Shukla 2003; Kodanova et al. 2019). For the parameters used in this work, this condition is always satisfied.

The explicit expression of the absorption current in the equilibrium is given by (de Juli & Schneider 1998)

$$I_{\beta 0}(q_\mathrm{d}) = \pi a^2 q_\beta \int \mathrm{d}^3 p \left(1 - \frac{C_\beta}{p^2}\right) H\left(1 - \frac{C_\beta}{p^2}\right) \frac{p}{m_\beta} f_{\beta 0}, \tag{4}$$

where m_β and $f_{\beta 0}$ are, respectively, the mass and the distribution function of the plasma species β in equilibrium, $H(x)$ is the Heaviside function, and

$$C_\beta \equiv \frac{2 q_\mathrm{d} q_\beta m_\beta}{a}. \tag{5}$$

The model for the photoionization current considers that radiation is unidirectional, striking only one side of the dust particle. When the energy of the radiation is greater than the work function of the material, electrons can be emitted. Its expression is given by (see Galvão & Ziebell 2012, appendix)

$$I_\mathrm{p} = \frac{2}{h^3} \int \mathrm{d}^3 p\, \sigma_\mathrm{p}(p, q_\mathrm{d}) \frac{p_z}{m_\mathrm{e}} \left[1 + \exp\left(\frac{p^2}{2 m_\mathrm{e} k_\mathrm{B} T_\mathrm{d}} - \xi\right)\right]^{-1}, \tag{6}$$

where h is the Planck constant, T_d is the dust temperature, and

$$\xi = \frac{1}{k_\mathrm{B} T_\mathrm{d}} (h\nu - \phi), \tag{7}$$

with ν being the incident radiation frequency, and ϕ the work function of the material. The photoemission cross-section is written as

$$\sigma_\mathrm{p}(p, q_\mathrm{d}) = e\, \pi a^2 \beta(\nu) \Lambda(\nu) H(p_z) H\left(1 - \frac{2 m_\mathrm{e} e q_\mathrm{d}}{a p^2} H(q_\mathrm{d})\right), \tag{8}$$

where e is the elementary charge, $\beta(\nu)$ is the probability of an electron that arrives to the surface coming from the inside to absorb a photon of frequency ν at the surface, and $\Lambda(\nu)$ is the number of photons with frequency ν incident per unit of area per unit of time.

If we consider that the star radiates as a blackbody, we can express the number of photons with frequency between ν and $\nu + \mathrm{d}\nu$ incident per unit time per unit area by

$$\Lambda(\nu)\, \mathrm{d}\nu = \frac{4\pi \nu^2}{c^2} \left[\exp\left(\frac{h\nu}{k_\mathrm{B} T_\mathrm{s}}\right) - 1\right]^{-1} \left(\frac{r_\mathrm{s}}{r_\mathrm{d}}\right)^2 \mathrm{d}\nu, \tag{9}$$

where c is the speed of light in vacuum, T_s is the surface temperature of the star, r_s is the radius of its radiating surface, and r_d is the mean distance of the dust grains from the star.

Both integrals in momenta appearing in equations (4) and (6) can be solved. More details on these charging models can be found in De Toni & Gaelzer (2021) where the absorption current is solved for Maxwellian distribution of plasma particles and the photoemission current is expressed in terms of empirical quantities, such as the maximum photoelectric efficiency χ_m of the material, and is generalized to the case of a continuous spectrum of the radiation.

As mentioned before, when writing the kinetic equations of the system, these charging processes will alter the equations for plasma particles. On top of that, one must also supply a kinetic equation for the dust population. Therefore, considering that dust particles are motionless and have all the same size, we can write the Vlasov–Maxwell set of equations as (Galvão & Ziebell 2012)

$$\frac{\partial f_\mathrm{d}}{\partial t} + \frac{\partial}{\partial q}(I f_\mathrm{d}) = 0, \tag{10}$$

$$\left(\frac{\partial}{\partial t} + \frac{\boldsymbol{p}}{m_\beta} \cdot \nabla_{\boldsymbol{r}} + q_\beta \left[\boldsymbol{E} + \frac{\boldsymbol{p}}{m_\beta c} \times \boldsymbol{B}\right] \cdot \nabla_{\boldsymbol{p}}\right) f_\beta = J_\beta + J_\mathrm{p}, \tag{11}$$

$$\nabla \cdot \boldsymbol{E} = 4\pi \sum_\beta q_\beta \int \mathrm{d}^3 p f_\beta + 4\pi \int \mathrm{d}q\, q f_\mathrm{d}(\boldsymbol{r}, q, t), \tag{12}$$

$$\nabla \cdot \boldsymbol{B} = 0, \tag{13}$$

$$\nabla \times \boldsymbol{E} = -\frac{1}{c} \frac{\partial \boldsymbol{B}}{\partial t}, \tag{14}$$

$$\nabla \times \boldsymbol{B} = \frac{1}{c} \frac{\partial \boldsymbol{E}}{\partial t} + \frac{4\pi}{c} \sum_\beta \frac{q_\beta}{m_\beta} \int \mathrm{d}^3 p\, \boldsymbol{p} f_\beta, \tag{15}$$

Downloaded from https://academic.oup.com/mnras/article/516/3/4650/6696011 by Universidade Federal do Rio Grande do Sul user on 02 December 2022

where I is the total current incident on dust grains, whilst $f_{\rm d}(\boldsymbol{r}, q, t)$ and $f_\beta(\boldsymbol{r}, \boldsymbol{p}, t)$ are, respectively, the distribution functions of dust and plasma particles of species β. The collisional integral J_β is closely related to the I_β current and acts as a sink of ions and electrons, since they are absorbed by dust grains. On the other hand, the term $J_{\rm p}$ describes a source of electrons that are emitted by the photoionization of dust particles and is related to the $I_{\rm p}$ current.

The postulation of immobile dust grains greatly simplifies the kinetic equation for the dust population since it excludes the momentum dependence of $f_{\rm d}$. However, as a consequence, it restricts the model to the range of wave frequencies much higher than the characteristic dust frequencies. That is, we must consider the regime in which $\omega \gg \max(\omega_{\rm d}, |\Omega_{\rm d}|)$, where $\omega_{\rm d}$ and $\Omega_{\rm d}$ are, respectively, the plasma and cyclotron frequencies of the dust particles. Hence, this model is not adequate to study wave modes that arise from dust dynamics, such as the dust acoustic waves, dust ion acoustic waves, and electrostatic dust ion cyclotron waves.

3 THE DIELECTRIC TENSOR AND DISPERSION RELATION FOR OBLIQUE ALFVÉN WAVES

Performing a linear approximation in the set of equations (10)–(15), where we assume that the fields and distribution functions can be written as a summation of an equilibrium part and a small perturbation, e.g. $f_\beta = f_{\beta 0} + f_{\beta 1}$, and using the Fourier transform of the perturbation, the dielectric tensor will have the form (Galvão & Ziebell 2012)

$$\epsilon_{ij} = \epsilon^{\rm C}_{ij} + \epsilon^{\rm A}_{ij} + \epsilon^{\rm P}_{ij}, \tag{16}$$

where $\epsilon^{\rm C}_{ij}$ indicates the components that have almost the same formal structure of a conventional (dustless) plasma. The terms $\epsilon^{\rm A}_{ij}$ and $\epsilon^{\rm P}_{ij}$ are related to the dust charging processes considered in the formalism, and would not appear in a dustless plasma. The former appears due to the absorption of plasma particles by the dust, whilst the latter is related to the photoionization of dust particles. As a first approach to the problem, we consider only the 'conventional' part of the dielectric tensor, i.e. we make $\epsilon_{ij} = \epsilon^{\rm C}_{ij}$.

Therefore, for a Maxwellian distribution of plasma particles, the dielectric tensor can be written as

$$\epsilon_{ij} = \delta_{ij} + \sum_{n=-\infty}^{\infty} \sum_{\beta} \frac{\omega^2_{{\rm p}\beta}}{\omega n_{\beta 0}} \int {\rm d}^3 p \left(\frac{p_\parallel}{p_\perp}\right)^{\delta_{jz}} \frac{\partial f_{\beta 0}}{\partial p_\perp} \times \frac{p_\parallel^{\delta_{iz}} p_\perp^{\delta_{ix}+\delta_{iy}} \Pi^{n\beta}_{ij}}{\omega - n\Omega_\beta - \frac{k_\parallel p_\parallel}{m_\beta} + {\rm i}\nu^0_{\beta {\rm d}}(p)}, \tag{17}$$

where ω is the angular frequency, $\omega_{{\rm p}\beta}$ and Ω_β are, respectively, the plasma and cyclotron frequencies of particles of species β. The tensor $\Pi^{n\beta}_{ij}$ is related to the Bessel functions and its first derivatives (see e.g. de Juli et al. 2005, appendix).

The presence of dust particles introduces a new imaginary term in the resonant denominator of equation (17), featuring the inelastic collision frequency $\nu^0_{\beta {\rm d}}(p)$ between dust and plasma particles. To evaluate the momentum integral, we replace this term by its average value in momentum space:

$$\nu_\beta = \frac{1}{n_{\beta 0}} \int {\rm d}^3 p \, \nu^0_{\beta {\rm d}}(p) f_{\beta 0}. \tag{18}$$

This procedure enable us to derive relatively simple expressions for the dispersion relation and it has been shown to be a good approximation in the frequency range of Alfvén waves (de Juli et al. 2007).

The dispersion relation for a homogeneous magnetized plasma with $\boldsymbol{B}_0 = B_0 \boldsymbol{e}_z$ and a wave vector $\boldsymbol{k}$ lying on the xz plane is given by

$$\det \begin{pmatrix} \epsilon_{xx} - N_\parallel^2 & \epsilon_{xy} & \epsilon_{xz} + N_\parallel N_\perp \\ \epsilon_{yx} & \epsilon_{yy} - N^2 & \epsilon_{yz} \\ \epsilon_{zx} + N_\parallel N_\perp & \epsilon_{zy} & \epsilon_{zz} - N_\perp^2 \end{pmatrix} = 0, \tag{19}$$

where $\boldsymbol{N} = N_\perp \boldsymbol{e}_x + N_\parallel \boldsymbol{e}_z = \boldsymbol{k}c/\omega$ is the refractive index.

We now introduce the following dimensionless parameters:

$$z = \frac{\omega}{\Omega_i}, \quad \varepsilon = \frac{n_{\rm d0}}{n_{\rm i0}}, \quad u_\beta = \frac{v_{{\rm T}\beta}}{v_{\rm A}}, \quad \chi_\beta = \frac{q_{\rm d0} q_\beta}{a k_{\rm B} T_\beta},$$
$$\gamma = \frac{\lambda^2 n_{\rm i0} v_{\rm A}}{\Omega_i}, \quad \tilde{a} = \frac{a}{\lambda}, \quad \lambda = \frac{e^2}{k_{\rm B} T_i}, \quad \boldsymbol{q} = \frac{\boldsymbol{k} v_{\rm A}}{\Omega_i},$$
$$\tilde{\nu}_\beta = \frac{\nu_\beta}{\Omega_i}, \quad \eta_\beta = \frac{\omega_{{\rm p}\beta}}{\Omega_i}, \quad r_\beta = \frac{\Omega_\beta}{\Omega_i}, \tag{20}$$

where $v_{\rm A}$ is the Alfvén velocity,

$$v_{\rm A}^2 = \frac{B_0^2}{4\pi n_{\rm i0} m_i}. \tag{21}$$

The group velocity, given the cylindrical symmetry and that $\boldsymbol{k}$ is lying on the xz plane, is expressed as

$$\boldsymbol{v}_{\rm g} = \frac{\partial \omega}{\partial k_\perp} \boldsymbol{e}_x + \frac{\partial \omega}{\partial k_\parallel} \boldsymbol{e}_z, \tag{22}$$

and, in terms of these dimensionless quantities, can be written as

$$\boldsymbol{u}_{\rm g} = \frac{\partial z}{\partial \boldsymbol{q}} = \frac{\boldsymbol{v}_{\rm g}}{v_{\rm A}}. \tag{23}$$

Considering that the studied modes have large wavelength in the perpendicular direction, i.e. $q_\perp \ll 1$, and keeping only the $n = -1$, 0, 1 harmonics in the dielectric components, the dispersion relation for obliquely propagating waves can be written as follows:

$$\begin{aligned} &\left[\left(\frac{z^2}{\eta_i^2} + \epsilon^1_{yy} - q_\parallel^2\right)\left(\frac{z^2}{\eta_i^2} + \epsilon^1_{xx} - q_\parallel^2\right) - (\epsilon^1_{xy})^2\right]\left(\frac{z^2}{\eta_i^2} + \epsilon^0_{zz}\right) \\ &+ \left\{\left(\frac{z^2}{\eta_i^2} + \epsilon^0_{zz}\right)\left(\frac{z^2}{\eta_i^2} + \epsilon^1_{xx} - q_\parallel^2\right)\left(\epsilon^0_{yy} - 1\right)\right. \\ &+ \left(\frac{z^2}{\eta_i^2} + \epsilon^1_{yy} - q_\parallel^2\right)\left[\left(\epsilon^1_{zz} - 1\right)\left(\frac{z^2}{\eta_i^2} + \epsilon^1_{xx} - q_\parallel^2\right)\right. \\ &\left. - \left(\epsilon^1_{xz} + q_\parallel\right)^2\right] - \left[-2\epsilon^1_{xy}\epsilon^1_{yz}\left(\epsilon^1_{xz} + q_\parallel\right)\right. \\ &\left.\left. + (\epsilon^1_{xy})^2\left(\epsilon^1_{zz} - 1\right) + (\epsilon^1_{yz})^2\left(\frac{z^2}{\eta_i^2} + \epsilon^1_{xx} - q_\parallel^2\right)\right]\right\} q_\perp^2 \\ &+ \left\{\left(\epsilon^0_{yy} - 1\right)\left[\left(\frac{z^2}{\eta_i^2} + \epsilon^1_{xx} - q_\parallel^2\right)\left(\epsilon^1_{zz} - 1\right)\right.\right. \\ &\left.\left. - \left(\epsilon^1_{xz} + q_\parallel\right)^2\right]\right\} q_\perp^4 = 0, \end{aligned} \tag{24}$$

where $\eta_i = c/v_{\rm A}$ and the $\epsilon^{0,1}_{ij}$ tensor components are related to the ϵ_{ij} components. A more detailed account of this derivation and explicit expressions for these components can be found in Gaelzer et al. (2009).

4 NUMERICAL RESULTS

To solve the dispersion relation we consider the same set of parameters used in previous works to study Alfvén waves within the kinetic theory (e.g. de Juli et al. 2005; Ziebell et al. 2005; Gaelzer et al. 2009, 2010; De Toni & Gaelzer 2021; De Toni et al. 2022), i.e.

Downloaded from https://academic.oup.com/mnras/article/516/3/4650/6696011 by Universidade Federal do Rio Grande do Sul user on 02 December 2022

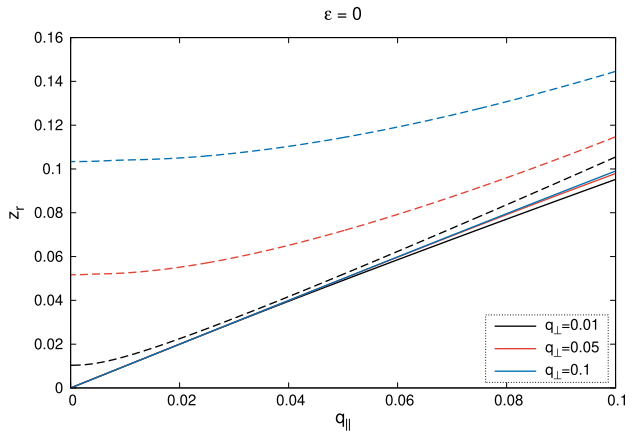

Figure 1. Real part of the normalized frequency z_r as a function of normalized wavenumber in the parallel direction $q_\parallel$ for several values of perpendicular wavenumber $q_\perp$ for a dustless plasma ($\varepsilon = 0$). Continuous lines correspond to SAW, whilst dashed lines correspond to the CAW.

$B_0 = 1$ G, $n_{i0} = 10^9$ cm^{-3}, $T_i = 10^4$ K, $T_e = T_i$, and $a = 10^{-4}$ cm. This set of parameters corresponds to values typically found in the winds of carbon-rich stars (Tsytovich, Morfill & Thomas 2004).

In this environment, dust particles are composed mainly of carbon (Nanni et al. 2021), for that reason, we choose the following values for the dust's physical parameters: work function $\phi = 4.6$ eV; maximum photoelectric efficiency $\chi_m = 0.05$; and dust temperature $T_d = 300$ K. The chosen value of T_d is within the range of dust temperatures in the inner circumstellar dust shells of carbon stars (Gail & Sedlmayr 2014).

To calculate the radiation flux from equation (9) we consider a distance of $r_d = 2\,r_s$, which is within the region of dust formation in dust-driven winds of carbon stars (Danchi et al. 1994; Gail & Sedlmayr 2014). Since we are dealing with the inner dust shells, we consider that there is no dust between the font and the studied region, so we may neglect the reddening effect of radiation that could occur as a result of the extinction of light caused by other dust particles.

The surface temperatures of carbon stars may vary widely from around $T_s = 2000$ to over 5000 K (Wallerstein & Knapp 1998). For the parameters used in this work, stars with temperatures above 3500 K start presenting significant effects on Alfvén waves caused by photoionization of dust particles, so that we choose to work with temperatures above this value in our numerical analysis.

We start our analysis by investigating the group velocity behaviour in a dustless plasma ($\varepsilon = 0$), solving the equation (24) using the parameters mentioned above. Fig. 1 shows the evolution of the real part of the normalized wave frequency z_r as a function of the parallel normalized wavenumber $q_\parallel$. The perpendicular wavenumber is considered a fixed parameter with values $q_\perp = 0.01$, 0.05, and 0.1, distinguished by the different line colours.

This figure is useful to identify the different wave modes that appear from the dispersion relation. Continuous lines represent the SAW for small wavenumber and become the ion cyclotron mode for large wavenumber. We can see that for small values of $q_\parallel$, this mode is not sensitive to the chosen value of $q_\perp$. It is only for larger $q_\parallel$ that is possible to see some small differences between the different line colours for the ion cyclotron mode.

On the other hand, the dashed lines present a greater sensitivity to changes in $q_\perp$. These lines identify the CAW for small wavenumber and become the whistler mode for large wavenumber. We notice that

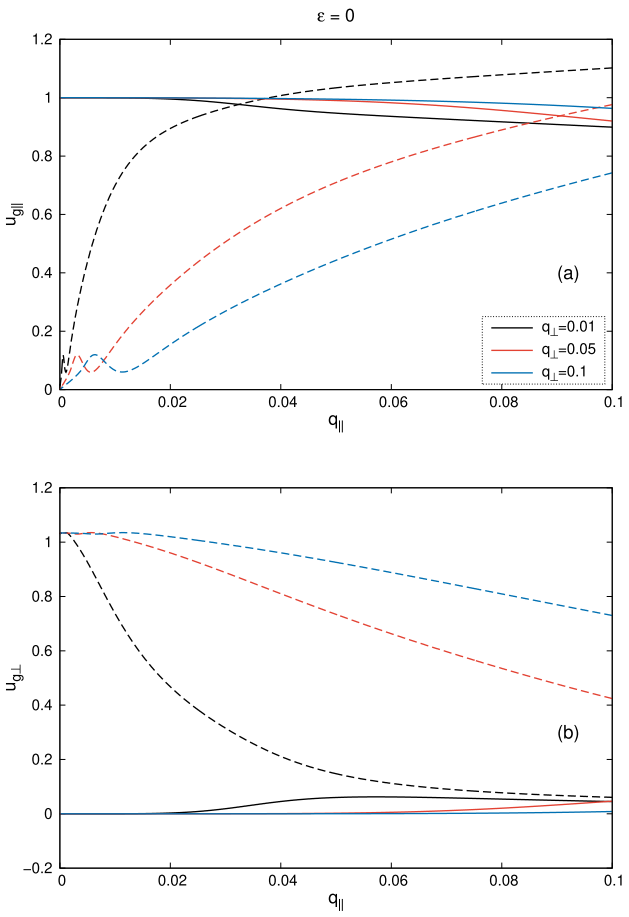

Figure 2. (a) Parallel and (b) perpendicular component of normalized group velocity u_g as functions of $q_\parallel$ for the wave modes presented in Fig. 1. Continuous lines are the SAW/ion cyclotron waves, whilst dashed lines are the CAW/whistler waves.

for very small $q_\parallel$, this mode approaches a non-zero value of wave frequency z_r, which decreases together with the $q_\perp$ parameter. For purely parallel propagation, the whistler wave approaches $z_r = 0$ for small wavenumber and couple with the ion cyclotron mode into a single wave mode in a dustless plasma (see e.g. de Juli et al. 2005; De Toni & Gaelzer 2021).

Now we look at the group velocity of these modes from the numerical differentiation of the dispersion relation. This is done by a simple two-point estimation:

$$\frac{f(x+h) - f(x)}{h}, \tag{25}$$

which gives the derivative of the function $f(x)$ in the limit of h approaching zero. However, from the computational point of view, the finite difference approximation of the derivative suffers from catastrophic cancellation for very small h, which restricts the practical use of the formula for h smaller than a critical value, corresponding to the greatest obtainable accuracy for the approximation.

Fig. 2 shows the parallel (top panel) and perpendicular (bottom panel) components of $\boldsymbol{u}_g = \boldsymbol{v}_g/v_A$, i.e. the derivative given by equation (23), which gives information about the velocity of a wave packet and energy propagation along and perpendicular to the magnetic field lines, for the modes presented in Fig. 1.

We see that the SAW/ion cyclotron waves (continuous lines) present parallel group velocity similar to the Alfvén velocity for

Downloaded from https://academic.oup.com/mnras/article/516/3/4650/6696011 by Universidade Federal do Rio Grande do Sul user on 02 December 2022

Table 1. Numerical values for the dust charge number Z_d for the parameters given in the beginning of this section. The left-hand side of the table shows the cases with constant stellar surface temperature $T_s = 3500$ K and several values of dust to ion density ratio ε, as studied in Fig. 3(a). The right-hand side corresponds to the curves in Fig. 3(b), with constant $\varepsilon = 5 \times 10^{-6}$ and varying T_s.

$T_s = 3500$ K		$\varepsilon = 5 \times 10^{-6}$	
ε	Z_d	T_s (K)	Z_d
10^{-7}	-1431	0	-1495
10^{-6}	-1430	3500	-1427
2.5×10^{-6}	-1429	4000	-1025
5.0×10^{-6}	-1427	4500	-205
7.5×10^{-6}	-1425	5000	$+349$
10^{-5}	-1424	5500	$+699$

small $q_\parallel$, whilst the perpendicular component is near zero in that region, regardless of their $q_\perp$ value. The group velocity of these modes only change slightly as the waves present higher values of $q_\parallel$.

However, the group velocity of CAW/whistler waves (dashed lines) displays larger changes as the wavenumber values are modified. The parallel component of group velocity presents higher values for increasing $q_\parallel$, with the exception of a short interval in the small $q_\parallel$ region in which $u_{g\parallel}$ decreases. The component $u_{g\perp}$, on the other hand, tends to decrease as $q_\parallel$ increases, more sharply for smaller values of $q_\perp$.

Furthermore, we notice that the values of $u_{g\perp}$ for SAW are much lower than $u_{g\parallel}$, which will also happen in the subsequent studies in this work (see Figs 6 and 8). This indicates that the wave energy is transported predominantly along the magnetic field lines, which is expected for this wave mode (Chen & Zonca 2014; Chen et al. 2021).

It is worth mentioning that Figs 1 and 2 present only the positive roots of the dispersion relation, which correspond to forward-propagating waves relative to the magnetic field. There are also negative solutions (see e.g. Gaelzer et al. 2009; De Toni et al. 2022), representing backward-propagating waves, with the same absolute values of z_r and u_g, but opposite signs. For the sake of clarity, we present only the solutions for forward-propagating waves throughout this work, keeping in mind that there are also solutions to the dispersion relation that are symmetric about the x-axis.

Now we look at the effects of dust particles on these wave modes. First of all, we observe that the dust particles will acquire an equilibrium electrical charge $q_{d0} = Z_d e$, where Z_d is the dust charge number, which will depend on the plasma parameters. Table 1 presents the values of the dust charge number utilizing the set of parameters previously discussed for several values of dust to ion density ε and radiation flux, given by the stellar surface temperature T_s.

We notice that by fixing T_s and varying ε, the charge number is almost not affected at all for the values considered. None the less, as we will see, the wave modes and its group velocities may present significant changes in their behaviour when we increase the dust density. This is due to the inelastic collision frequency that appears in the resonant denominator of equation (17), which is affected by this parameter.

On the other hand, the dust charge number in Table 1 is significantly altered by varying T_s, to the point where dust particles become positively charged, a consequence of the photoionization process. In this case, the inelastic collision frequency will be altered especially by the changes in the equilibrium dust charge and in the electron density, since the changes in the dust electrical charge will

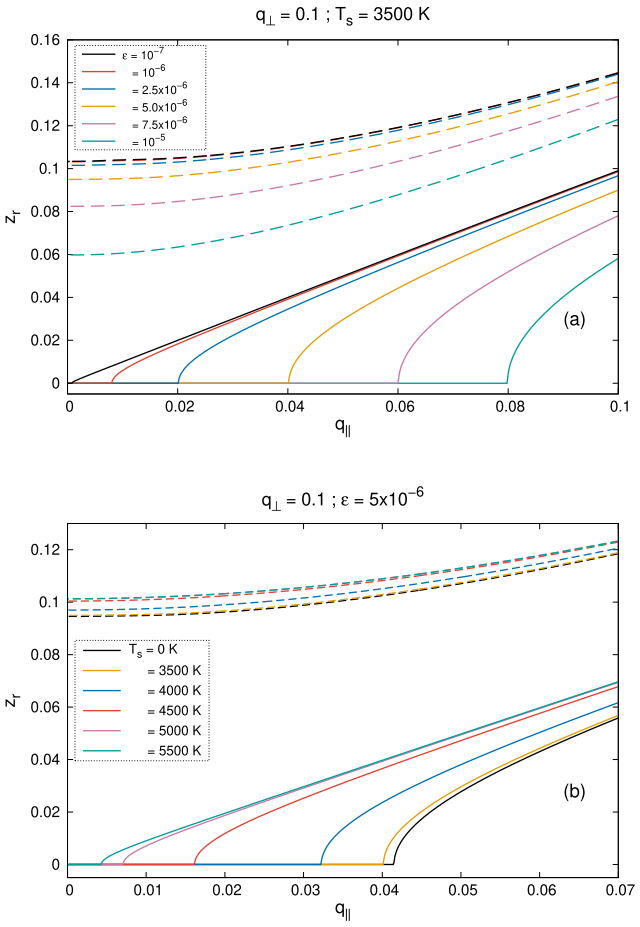

Figure 3. Real part of the normalized frequency z_r as a function of normalized parallel wavenumber $q_\parallel$ and fixed $q_\perp = 0.1$ for: (a) fixed value of stellar surface temperature $T_s = 3500$ K and several values of dust to ion density ratio ε; (b) fixed $\varepsilon = 5 \times 10^{-6}$ and varying the value of T_s. Dashed and continuous lines represent, respectively, the forward-propagating CAW/whistler modes and the SAW/ion cyclotron modes.

also modify the plasma particles densities by the quasi-neutrality condition (see equation 3).

Fig. 3 displays the forward-propagating wave modes that appear for the set of parameters previously discussed. As before, the dashed and continuous lines represent, respectively, the CAW and SAW. By fixing the value of $q_\perp = 0.1$, we observe that when the dust to ion density ratio ε is not zero, the SAWs present a region of null z_r. This non-propagating region appears in the presence of dust particles and was already studied in the works of Gaelzer et al. (2009) and De Toni et al. (2022). The results show that the interval of $q_\parallel$ where the real frequency is zero is decreased for smaller dust density (top panel) and for higher radiation flux (bottom panel).

We now look to the group velocities of each mode separately in both cases, varying dust density and varying the radiation flux. Figs 4 and 5 show the parallel (top panels) and perpendicular (bottom panels) components of the group velocity of the CAW/whistler modes presented in Fig. 3. We notice that the behaviour of the group velocity for small dust density is very similar to what is observed for a dustless plasma, in Fig. 2, with $u_{g\parallel}$ still presenting decreasing values for a short interval of $q_\parallel$ values (around $0.005 \lesssim q_\parallel \lesssim 0.01$). However, Figs 4(a) and 5(a) show that this feature tends to disappear for higher

Downloaded from https://academic.oup.com/mnras/article/516/3/4650/6696011 by Universidade Federal do Rio Grande do Sul user on 02 December 2022

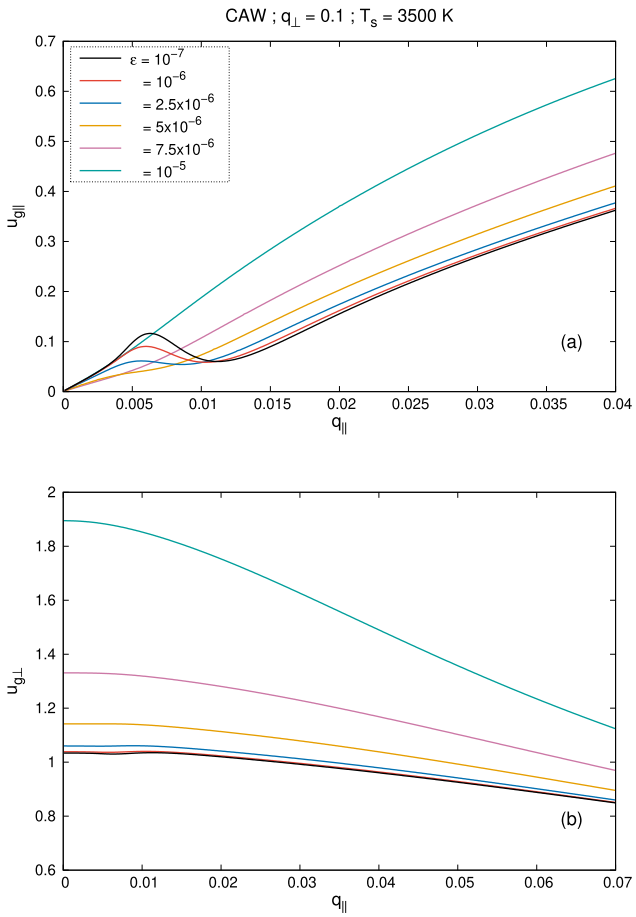

Figure 4. (a) Parallel and (b) perpendicular component of normalized group velocity u_g as functions of $q_\parallel$ for the CAWs presented in Fig. 3(a), with constant stellar surface temperature $T_s = 3500$ K and several values of dust to ion density ratio ε.

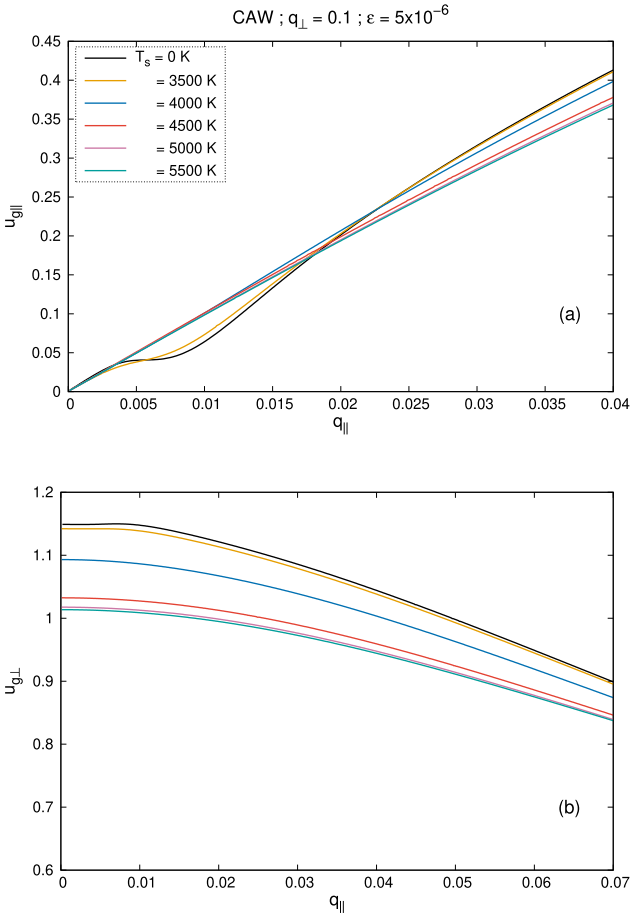

Figure 5. (a) Parallel and (b) perpendicular component of normalized group velocity u_g as functions of $q_\parallel$ for the CAWs presented in Fig. 3(b), with constant dust to ion density ratio $\varepsilon = 5 \times 10^{-6}$ and several values of stellar surface temperature T_s.

values of dust density or radiation flux, with $u_{g\parallel}$ monotonically increasing in all interval of $q_\parallel$ studied.

The perpendicular component $u_{g\perp}$ of CAWs also shows little changes for small dust density when compared to the dustless plasma case. Figs 4(b) and 5(b) show that the values of $u_{g\perp}$ tends to increase in cases with higher values of ε or smaller values of T_s. For instance, a dust to ion density ratio of $\varepsilon = 10^{-5}$ may cause the perpendicular group velocity of waves with small $q_\parallel$ to achieve values almost two times bigger than the Alfvén velocity, for the parameters considered, indicating that the propagation of the wave packet for small $q_\parallel$ will occur at greater angles from the magnetic field for higher dust density.

The group velocity values of the SAWs displayed in Fig. 3(a) are presented in Fig. 6. Both parallel (top panel) and perpendicular (bottom panel) components of u_g show null values in the region where these modes have zero frequency z_r. At the point in which the modes become dispersive, we notice a jump of the group velocity from zero to a finite value, causing a discontinuity in the plot, and starts decreasing afterwards.

This value of the group velocity at the point of discontinuity is not well defined by our numerical method since the ion cyclotron curves in Fig. 3 indicate that the derivative at the point in which they no longer present $z_r = 0$ tends to infinity (similarly to the behaviour of a square root function at the origin). For that reason, the value of u_g at this point becomes dependent of the step h utilized in equation (25), as is illustrated in Fig. 7.

None the less, all numerical derivatives presented in Fig. 7 show similar values of $u_{g\parallel}$ outside the vicinity of the discontinuity point. Anyhow, the fact that u_g tends to infinity indicates that the group velocity in that spectral region does not have physical significance as the velocity of propagation of a wave packet, as it occurs in regions of anomalous dispersion (see e.g. Brillouin 1960).

Back to Fig. 6, we see that the parallel group velocity of SAWs starts decreasing after the point of discontinuity, converging to values near the Alfvén velocity ($u_{g\parallel} = 1$). The perpendicular component has values significantly lower and shows a distinct behaviour for some ε values, with negative $u_{g\perp}$ right after the discontinuity point, i.e. in a small range of $q_\parallel$, the perpendicular group velocity for these waves is in opposite direction to the perpendicular phase velocity.

This region of negative $u_{g\perp}$ is rather small, turning into positive values for slightly bigger $q_\parallel$. For small dust density this feature does not appear, with the group velocity presenting positive values for all $q_\parallel$, as can be seen in the zoomed-in boxes in Fig. 6(b) for the $\varepsilon = 10^{-6}$ and 10^{-7} curves.

The situation in which dust density is maintained fixed and the radiation flux is changed through the stellar surface temperature T_s is shown in Fig. 8 for SAW and same set of parameters as in Fig. 3(b). The behaviour of the parallel component of group velocity is very

Downloaded from https://academic.oup.com/mnras/article/516/3/4650/6696011 by Universidade Federal do Rio Grande do Sul user on 02 December 2022

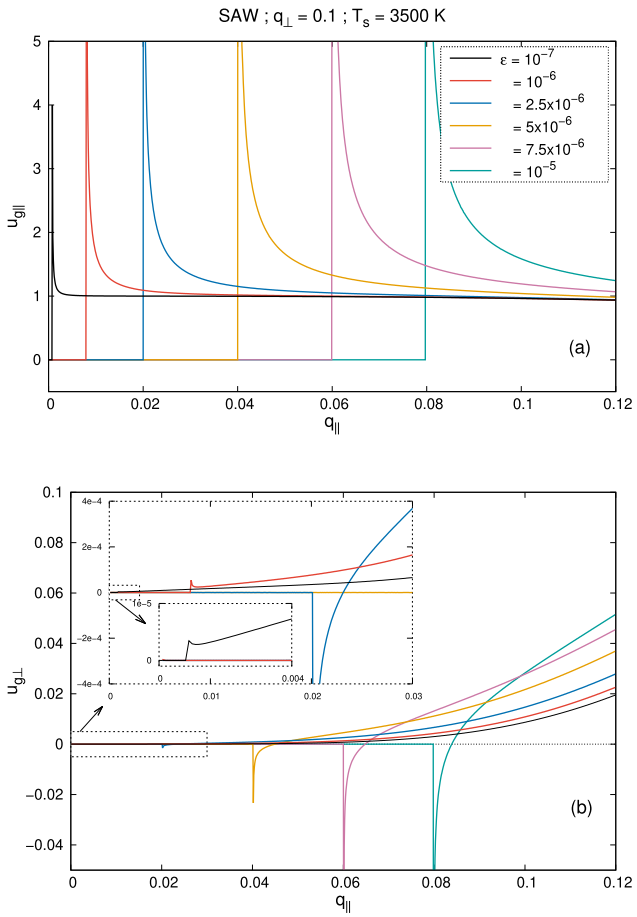

Figure 6. (a) Parallel and (b) perpendicular component of normalized group velocity u_g as functions of $q_\parallel$ for the SAWs presented in Fig. 3(a), with constant stellar surface temperature $T_s = 3500$ K and several values of dust to ion density ratio ε.

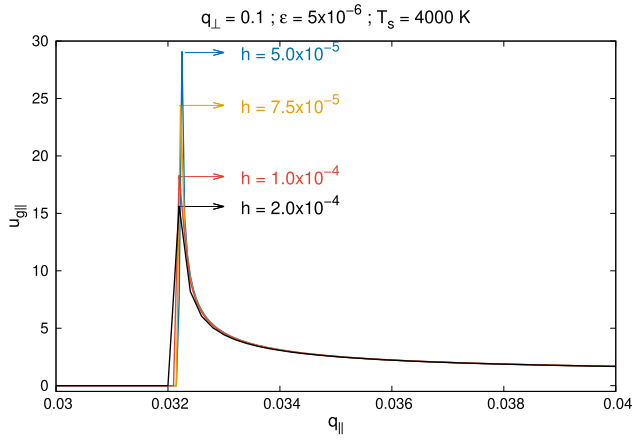

Figure 7. Parallel component of u_g for SAW as a function of $q_\parallel$ for distinct values of the step h utilized in the numerical differentiation (equation 25).

similar to what is observed in Fig. 6(a), with $u_{g\parallel}$ showing a region of anomalous dispersion at the point where the modes start presenting non-zero values of z_r, and decreasing to a value near the Alfvén velocity outside the vicinity of the discontinuity point.

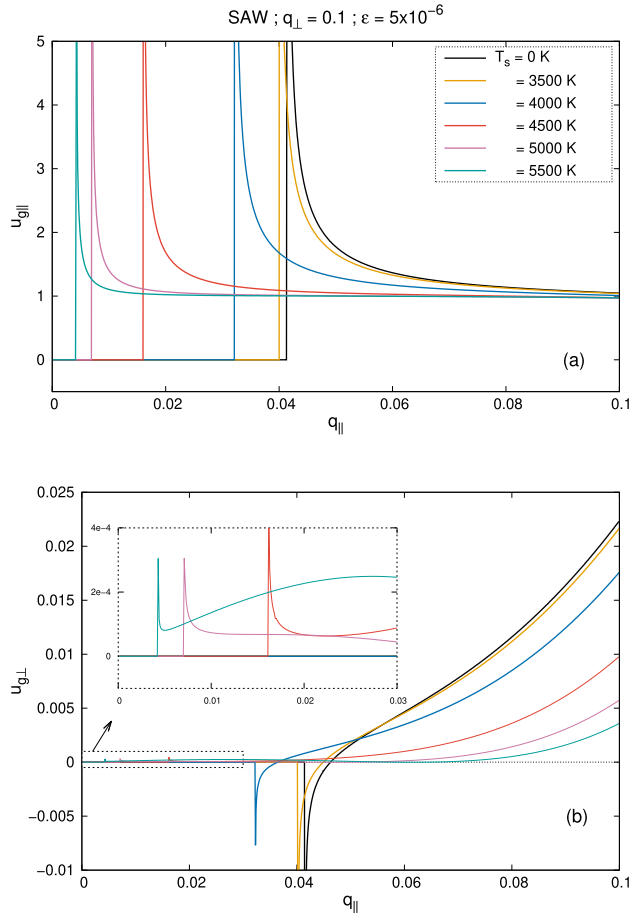

Figure 8. (a) Parallel and (b) perpendicular component of normalized group velocity u_g as functions of $q_\parallel$ for the SAWs presented in Fig. 3(b), with constant dust to ion density ratio $\varepsilon = 5 \times 10^{-6}$ and several values of stellar surface temperature T_s.

The perpendicular component $u_{g\perp}$ of these modes presents, as before, much smaller values than the parallel component and situations with negative values in a short interval of $q_\parallel$ near the point of discontinuity, for small radiation flux. For greater values of T_s, the perpendicular group velocity is positive (see zoomed-in box in bottom panel) right after the discontinuity point, as occurs with the parallel component.

However, we notice in some situations that $u_{g\perp}$ presents a complex behaviour and may even decrease to negative values in a short interval of $q_\parallel$, and become positive again. This can be visualized in Fig. 9, in which several other values of T_s have been added, in order to better show the transition of a curve with positive values for all $q_\parallel$ ($T_s \lesssim 4800$ K) to the cases showing negative $u_{g\perp}$ in some region ($T_s \gtrsim 5000$ K).

5 CONCLUSIONS

The characteristics of the group velocity of Alfvén waves propagating obliquely to the direction of the ambient magnetic field in a homogeneous dusty plasma are investigated. For that, we used a kinetic formulation that considers Maxwellian distributions for ions and electrons, and immobile dust particles. The dust grains are considered to have same radius and are charged by the absorption of plasma particles via inelastic collisions, and by photoionization due

Downloaded from https://academic.oup.com/mnras/article/516/3/4650/6696011 by Universidade Federal do Rio Grande do Sul user on 02 December 2022

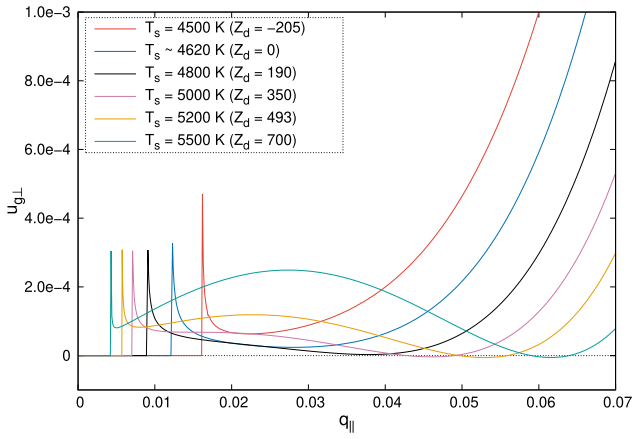

Figure 9. Perpendicular component of normalized group velocity u_g as function of $q_\parallel$ for the SAWs, with constant dust to ion density ratio $\varepsilon = 5 \times 10^{-6}$, $q_\perp = 0.1$, and several values of stellar surface temperature T_s, along with their corresponding dust charge number Z_d.

to the radiation flux coming from the star's surface. The parameters considered are typical of a stellar wind from a carbon-rich star.

The study is performed for the normal wave modes that arise from the dispersion relation, namely the CAW (or whistler, for large wavenumber) and SAW (or ion cyclotron). We observe the changes in the modes' normalized group velocity u_g along and transverse to the magnetic field by varying parameters related to the dust population, such as dust to ion number density ratio and equilibrium electrical charge of the dust grains (by varying the radiation flux via the stellar surface temperature).

The results show that, for a fixed transverse component of the normalized wavenumber q, the parallel group velocity of CAWs generally increases with $q_\parallel$, whilst its perpendicular component decreases, i.e. the direction of the wave packet propagation is greatly modified with the wave-vector direction. We also noticed that, for small $q_\parallel$, the increase of dust number density can greatly increase the $u_{g\perp}$ values whilst maintaining $u_{g\parallel}$ almost constant, indicating that in dusty plasmas these waves with large wavelength will propagate energy at greater angles relative to the magnetic field, in comparison with conventional plasmas.

SAWs, on the other hand, will generally present much higher values of $u_{g\parallel}$, consequence of its anisotropic nature, with group velocity propagating practically along the magnetic field. Nevertheless, when these waves have non-zero frequency, its perpendicular component shows to be non-vanishing and, for sufficiently high values of dust number density, it may present negative values in a small interval of $q_\parallel$. This interval with negative $u_{g\perp}$ may be modified, or even vanish, by changes in the radiation flux incident on the dust particles, which modifies the grains' equilibrium electrical charge.

From this study and from the previous publication (De Toni et al. 2022), it is seen that obliquely propagating Alfvén waves are significantly changing their properties in a magnetized dusty plasma with the modification of dust-related parameters. These findings may prove to be helpful in better understanding plasma heating and energy flux processes in stellar wind environments, since the plasma parameters in these places could be greatly modified by the presence of dust. For instance, waves generated within different distances from the star's radiating surface will have distinct characteristics, given that dust number density and radiation flux are dependent of the distance from the star.

Further studies can be followed from this work. Our model incorporates only one population of dust grains with constant size. However, it is expected that space dusty plasmas present several dust populations with different sizes, with radii varying from about 10^{-4} to 10^{-7} cm in a dust-driven wind (Krüger & Sedlmayr 1997). The work of Galvão & Ziebell (2012) included, within the kinetic theory, a discrete distribution of grain sizes to derive an expression of the dielectric tensor for a magnetized dusty plasma. In the near future, we intend to make use of that formalism to incorporate a continuous distribution of grain sizes to our model, given that in space environments the dust radii are often described by a continuous distribution function (see e.g. Mathis, Rumpl & Nordsieck 1977; Dominik, Gail & Sedlmayr 1989; Hoefner & Dorfi 1992).

Moreover, our model does not take into account non-linear effects of the system. The development of a quasi-linear theory for a dusty plasma would allow to include the dynamical evolution of the grains' electrical charge in a self-consistent way in the kinetic theory. Also, a better understanding of the wave–particle and wave–wave interactions could be accomplished by a non-linear treatment, such as the weak turbulence theory of plasmas (Galvão & Ziebell 2015). These non-linear kinetic processes are believed to be important in the mechanism responsible for the heating and acceleration of stellar winds (De Pontieu et al. 2007; Cranmer et al. 2015; Raouafi et al. 2021). We also intend to pursue this line of investigation.

ACKNOWLEDGEMENTS

This study was financed in part by the Coordenação de Aperfeiçoamento de Pessoal de Nível Superior – Brasil (CAPES) – Finance Code 001. RG acknowledges support from CNPq (Brazil), grant no. 307845/2018-4. LFZ acknowledges support from CNPq (Brazil), grant no. 302708/2018-9.

DATA AVAILABILITY

The data underlying this paper will be shared on reasonable request to the corresponding author.

REFERENCES

Alazraki G., Couturier P., 1971, A&A, 13, 380
Allen J. E., 1992, Phys. Scr., 45, 497
Bale S. D., Kellogg P. J., Mozer F. S., Horbury T. S., Reme H., 2005, Phys. Rev. Lett., 94, 215002
Barnes A., 1969, ApJ, 155, 311
Belcher J. W., 1971, ApJ, 168, 509
Belcher J. W., Davis L., Jr, 1971, J. Geophys. Res., 76, 3534
Bellan P. M., 1994, Phys. Plasmas, 1, 3523
Bian N. H., Kontar E. P., Brown J. C., 2010, A&A, 519, A114
Boulangier J., Clementel N., van Marle A. J., Decin L., de Koter A., 2018, MNRAS, 482, 5052
Bowen G. H., 1988, ApJ, 329, 299
Brillouin L., 1960, Wave Propagation and Group Velocity. Academic Press, New York
Chang J. S., Spariosu K., 1993, J. Phys. Soc. Jpn., 62, 97
Chen L., Hasegawa A., 1974, Phys. Fluids, 17, 1399
Chen L., Zonca F., 1995, Phys. Scr., 60, 81
Chen L., Zonca F., 2014, JPS Conf. Proc., 1, 011001
Chen L., Zonca F., Lin Y., 2021, Rev. Mod. Plasma Phys., 5, 1
Cramer N. F., 2001, The Physics of Alfvén Waves. Wiley-VCH, Weinheim, Germany
Cranmer S. R., Asgari-Targhi M., Miralles M. P., Raymond J. C., Strachan L., Tian H., Woolsey L. N., 2015, Philos. Trans. R. Soc. A: Math. Phys. Eng. Sci., 373, 20140148

Downloaded from https://academic.oup.com/mnras/article/516/3/4650/6696011 by Universidade Federal do Rio Grande do Sul user on 02 December 2022

Danchi W. C., Bester M., Degiacomi C. G., Greenhill L. J., Townes C. H., 1994, AJ, 107, 1469
de Juli M. C., Schneider R. S., 1998, J. Plasma Phys., 60, 243
de Juli M. C., Schneider R. S., Ziebell L. F., Jatenco-Pereira V., 2005, Phys. Plasmas, 12, 052109
de Juli M. C., Schneider R. S., Ziebell L. F., Gaelzer R., 2007, Phys. Plasmas, 14, 022104
De Pontieu B. et al., 2007, Science, 318, 1574
De Toni L. B., Gaelzer R., 2021, MNRAS, 508, 340
De Toni L. B., Gaelzer R., Ziebell L. F., 2022, MNRAS, 512, 1795
Dominik C., Gail H. P., Sedlmayr E., 1989, A&A, 223, 227
Dürst J., 1982, A&A, 112, 241
Falceta-Gonçalves D., Jatenco-Pereira V., 2002, ApJ, 576, 976
Gaelzer R., de Juli M. C., Schneider R. S., Ziebell L. F., 2009, Plasma Phys. Controlled Fusion, 51, 015011
Gaelzer R., de Juli M. C., Ziebell L. F., 2010, J. Geophys. Res.: Space Phys., 115, A09109
Gail H.-P., Sedlmayr E., 2014, Physics and Chemistry of Circumstellar Dust Shells. Cambridge Univ. Press, Cambridge
Galvão R. A., Ziebell L. F., 2012, Phys. Plasmas, 19, 093702
Galvão R. A., Ziebell L. F., 2015, Phys. Rev. E, 92, 023102
Goertz C. K., Boswell R. W., 1979, J. Geophys. Res.: Space Phys., 84, 7239
Goldstein B. E., Smith E. J., Balogh A., Horbury T. S., Goldstein M. L., Roberts D. A., 1995, Geophys. Res. Lett., 22, 3393
Hasegawa A., 1976, J. Geophys. Res., 81, 5083
Hasegawa A., Chen L., 1976, Phys. Fluids, 19, 1924
Heinemann M., Olbert S., 1980, J. Geophys. Res., 85, 1311
Heyvaerts J., Priest E. R., 1983, A&A, 117, 220
Hoefner S., Dorfi E. A., 1992, A&A, 265, 207
Howard R. A. et al., 2019, Nature, 576, 232
Hui C.-H., Seyler C., 1992, J. Geophys. Res.: Space Phys., 97, 3953
Jatenco-Pereira V., Opher R., 1989, A&A, 209, 327
Keiling A. et al., 2002, J. Geophys. Res.: Space Phys., 107, SMP 24
Knapp G. R., 1987, in Kwok S., Pottasch S. R., eds, Late Stages of Stellar Evolution. Reidel, Dordrecht, p. 103
Kodanova S. K., Bastykova N. K., Ramazanov T. S., Nigmetova G. N., Maiorov S. A., Moldabekov Z. A., 2019, IEEE Trans. Plasma Sci., 47, 3052
Krüger D., Sedlmayr E., 1997, A&A, 321, 557
Lafon J.-P. J., Berruyer N., 1991, A&AR, 2, 249
Leamon R. J., Smith C. W., Ness N. F., Matthaeus W. H., Wong H. K., 1998, J. Geophys. Res.: Space Phys., 103, 4775
Leamon R. J., Smith C. W., Ness N. F., Wong H. K., 1999, J. Geophys. Res.: Space Phys., 104, 22331
Leamon R. J., Matthaeus W. H., Smith C. W., Zank G. P., Mullan D. J., Oughton S., 2000, ApJ, 537, 1054
Leinert C. et al., 1998, A&AS, 127, 1
Léna P., Viala Y., Hall D., Soufflot A., 1974, A&A, 37, 81
Lysak R., Song Y., Jones T., 2009, Ann. Geophys., 27, 2237
Malovichko P. P., 2013, Kinematics Phys. Celest. Bodies, 29, 269
Mankin W., MacQueen R., Lee R., 1974, A&A, 31, 17
Mathis J. S., Rumpl W., Nordsieck K. H., 1977, ApJ, 217, 425
Mattsson L., Höfner S., 2011, A&A, 533, A42
Nanni A., Cristallo S., van Loon J. T., Groenewegen M. A., 2021, Universe, 7, 233
Raouafi N. E., Vourlidas A., Zhang Y., Paxton L. J., eds, 2021, Space Physics and Aeronomy, Vol. 1, Solar Physics and Solar Wind. Wiley, New York
Salimullah M., Sandberg I., Shukla P. K., 2003, Phys. Rev. E, 68, 027403
Sandin C., Höfner S., 2003, A&A, 398, 253
Smith E. J., Balogh A., Neugebauer M., McComas D., 1995, Geophys. Res. Lett., 22, 3381
Stasiewicz K. et al., 2000, Space Sci. Rev., 92, 423
Swanson D. G., 2003, Plasma Waves, 2nd edn. Taylor & Francis, Oxfordshire, UK
Tomczyk S., McIntosh S. W., Keil S. L., Judge P. G., Schad T., Seeley D. H., Edmondson J., 2007, Science, 317, 1192
Tsytovich V. N., 1997, Soviet Phys. Uspekhi, 40, 53
Tsytovich V. N., Morfill G. E., Thomas H., 2004, Plasma Phys. Rep., 30, 816
Vásconez C. L., Pucci F., Valentini F., Servidio S., Matthaeus W. H., Malara F., 2015, ApJ, 815, 7
Wallerstein G., Knapp G. R., 1998, ARA&A, 36, 369
Woitke P., 2006, A&A, 452, 537
Ziebell L. F., de Juli M. C., Schneider R. S., Jatenco-Pereira V., 2005, Phys. Plasmas, 12, 082102
Ziebell L. F., Schneider R. S., de Juli M. C., Gaelzer R., 2008, Brazilian J. Phys., 38, 297

This paper has been typeset from a TEX/LATEX file prepared by the author.

Downloaded from https://academic.oup.com/mnras/article/516/3/4650/6696011 by Universidade Federal do Rio Grande do Sul user on 02 December 2022